ELSEVIER

Journal of Molecular Catalysis A: Chemical 1446 (1997) 119 (1997) 235–244

JOURNAL OF MOLECULAR CATALYSIS A: CHEMICAL

Cluster size effects in models of the active site for stereospecific heterogeneous Ziegler–Natta polymerization

David H. Mosley *, Caroline Denil, Benoît Champagne [1], Jean-Marie André

Laboratoire de Chimie Théorique Appliquée, Facultés Universitaires Notre-Dame de la Paix, Rue de Bruxelles 61, B-5000 Namur, Belgium

Received 4 June 1996; accepted 8 July 1996

Abstract

The extended Hückel molecular orbital method has been used to study models of the active site for Ziegler–Natta catalyzed olefin polymerization on the surface of crystalline $TiCl_3$ containing from one to twenty titanium atoms, and the coordination of an ethylene monomer by the active site. Significant differences are observed in the coordination of ethylene to the small model systems compared to the larger model systems. These differences are analyzed using the complexation energies, bond orders and orbital populations, and are interpreted in terms of back donation from low-lying d-orbitals of the active site to the π^* orbital of the olefin. Conclusions are drawn on the basis of these results regarding the requirements of model active sites suitable for study with more sophisticated theoretical methods.

Keywords: Extended Hückel calculations; Ziegler–Natta catalysis; Olefin polymerization; $TiCl_3$

1. Introduction

The Ziegler–Natta catalysis of the polymerization of olefins is of great industrial significance. In the forty years since its discovery, major advances have been made with regards to the improvement of the activity of the catalytic systems, control over the molecular weight distribution of the polymer, and the regio- and stereospecificity of the reaction [1,2].

The most widely accepted mechanism for Ziegler–Natta polymerization is due to Cossee [3]. This is a monometallic mechanism in which the initial step is the coordination of the olefin monomer to a vacant site of a metal–alkyl (the growing chain) complex. Subsequently, the olefin is inserted into the metal–alkyl bond via a four-center transition state. This creates a new vacancy in the metal–alkyl complex, and the polymerization can thus continue. Our interest here is olefin polymerization using heterogeneous titanium chloride based catalysts, following models of the catalytic sites on surfaces of α-$TiCl_3$ described by Corradini [4,5]. The $TiCl_3$ crystal structure is built of layers, with the titanium atoms in each layer occupying two-thirds of the octahedral positions, and neighboring titanium atoms are bridged by two chlorine atoms. A cut in a $TiCl_3$ layer parallel to bridged

* Corresponding author.

[1] Research Associate of the Belgian National Fund for Scientific Research (FNRS).

PII S1381-1169(96)00487-6

titanium atoms produces titanium atoms at the surface which are bonded to five chlorine atoms in a square-planar arrangement, and a vacant site. Of the five chlorine atoms, four are bridged to neighboring metal atoms, and the fifth is less strongly bound and can be substituted by an alkyl group, using an alkyl aluminium cocatalyst, to form the active site.

Many theoretical studies have been dedicated to the mechanism of Ziegler–Natta polymerization. Amongst the first of these, Armstrong et al. [6] used the semi-empirical CNDO method to investigate the Cossee mechanism for the catalytic system $Cl_2Al(\mu\text{-}Cl_2)$–$TiCl_2(CH_3)$ + C_2H_4. The first ab initio restricted Hartree–Fock (RHF) study of the reaction [7] used a similar catalytic system $((CH_3)_2Al(\mu\text{-}Cl_2)$–$TiCl_2(CH_3) + C_2H_4)$. These works suggested that the Ti–ethylene bond in the initial coordination step is weak, and the latter gave an estimation for the energy of activation for the olefin insertion to be of the order of 15 kcal mol^{-1}. More recently, Jensen et al. [8] improved significantly upon these earlier studies using full gradient geometry optimizations and reaction path calculations at the SCF level for ethylene insertion into the titanium–methyl bond in $H_2Al(\mu\text{-}Cl_2)$–$TiCl_2(CH_3)$. Electron correlation was taken into account at important stationary points on the potential energy surface (PES) calculated at the SCF level. The PES at steps along the reaction path prior to the transition state for ethylene was found to be almost flat (i.e. absence of a barrier) at the correlated level. The energy then decreases along the reaction path after this point resulting in an enthalpy of -21.9 kcal mol^{-1} for the full reaction.

In recent years, the majority of studies of olefin polymerization have focussed on using homogeneous titanocene and zirconocene catalysts. From the theoretical point of view, these systems have the advantage that they are well defined compared to heterogeneous systems. Reported calculations on model metallocenes have employed many methods, such as non-bonded potential energies to account for the stereo- and regiospecificity of olefin polymerization [9–11], semi-empirical PRDDO [12], ab initio Hartree–Fock [12–14], second order Møller–Plesset perturbation theory [12–14], and density functional [13–16] studies of the insertion reaction, and the ground-breaking ab initio molecular dynamics study of the metallocene-catalyzed polymerization of ethylene by Meier et al. [17].

For heterogeneous $TiCl_3$-based catalysis, the situation is more demanding. Although the chain growth takes place at a specific site, the influence of neighboring atoms in the crystal cannot be neglected. Accurate modelling of catalytic reactions on crystal surfaces using finite clusters is highly dependent upon the model system being able to reproduce correctly the electronic and steric environment in the bulk. The computational demands of ab initio methods limit the size of system which can be considered, hence it is of importance to develop small models which faithfully reproduce the characteristics of the active site in the crystal. Corradini and his co-workers [4,5] used non-bonded energies to rationalize the stereospecificity of the polymerization of propylene at active sites on the surface of α-$TiCl_3$. While this provides valuable insight, it is purely qualitative, failing to take into account electronic effects and assuming fixed geometries. Jensen [18] has reported ab initio calculations of the coordination of ethylene to square-planar models of the active sites, TiX_5^{n-} ($X = H$, F, Cl; $n = 1$, 2). The results show that the interaction between the olefin and the active site is weak, and that relaxation of the square-planar system to a trigonal-bipyrimidal geometry is preferable energetically to coordination of the monomer. This suggests that the rigid environment imposed on the active site in the crystal has an important role to play.

In this paper we apply the extended Hückel molecular orbital method to the study of the electronic characteristics of the active sites in models of the $TiCl_3$ crystalline surface of increasing size, and the initial step of the catalytic

reaction, the coordination of an ethylene monomer. The method is simple computationally, and allows us to consider realistic models of the $TiCl_3$ crystalline surface. The goal of our calculations is to use the information gained in the design of small models of the active site, possessing the characteristics of an active site on the crystal surface, but of a size suitable for treatment at higher levels of theory.

In Section 2 we describe the model clusters studied and give details regarding the calculation of the Giambiagi–Mayer bond orders [19,20] used in the analysis of the active site–olefin coordination step. We then present the results for the active site models and the interaction with an ethylene monomer before making some concluding remarks.

2. Methodology

2.1. Model active sites on the $TiCl_3$ crystal surface

Two types of model active sites are considered in this work, designated as *edge* and *corner*-type active sites, containing from one to twenty titanium atoms, with successive clusters differing by a $TiCl_3$ unit. All clusters were assumed to be uncharged. These models of the active sites are similar to those used by Shiga [21] in a recent extended Hückel and paired interacting orbital study of ethylene polymerization, although the largest system considered was limited to five titanium atoms. Figs. 1 and 2 show the edge and corner type sites, respec-

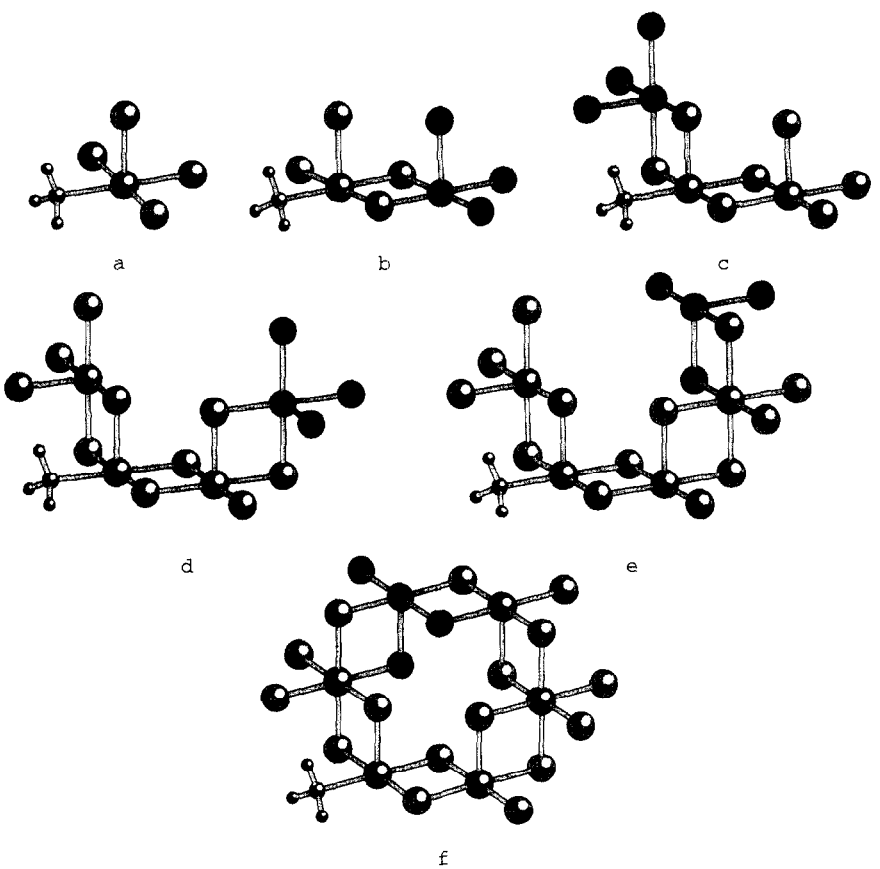

Fig. 1. Edge-type active site models on the surface of α-$TiCl_3$ of increasing size from $TiCl_4CH_3$ to $Ti_6Cl_{19}CH_3$. Successive models differ by a $TiCl_3$ unit, indicated by the darkest atoms in the figure.

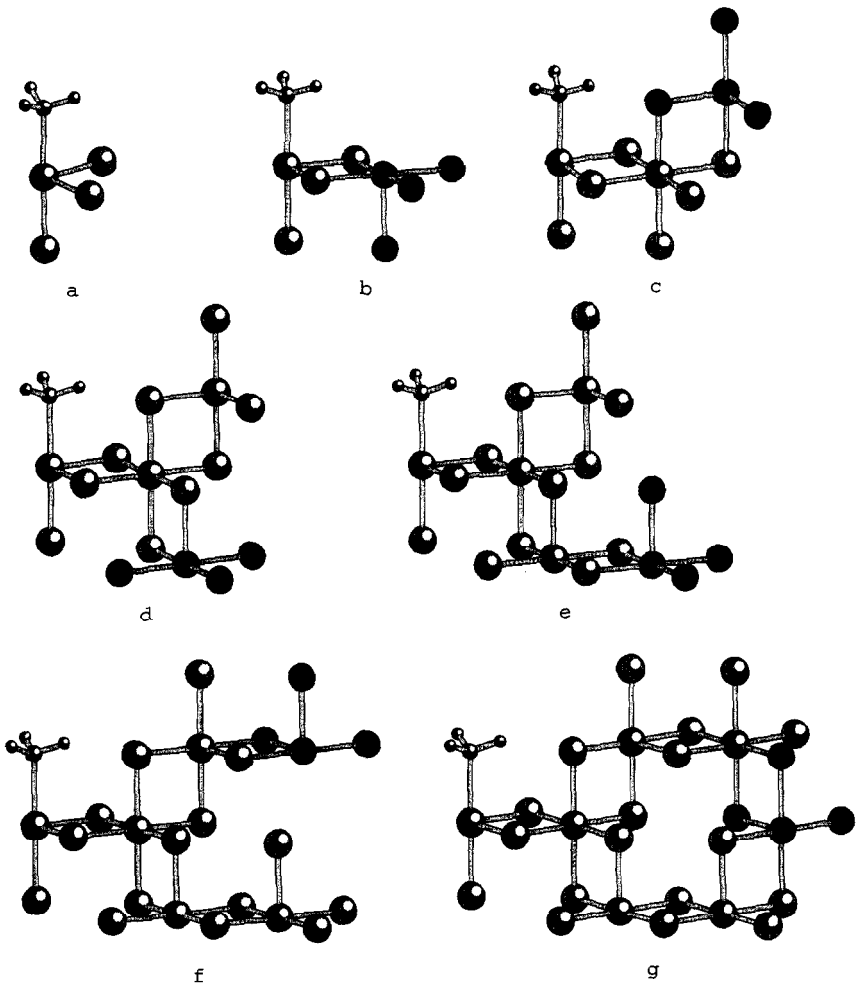

Fig. 2. Corner-type active site models on the surface of α-$TiCl_3$ of increasing size from $TiCl_3CH_3$ to $Ti_6Cl_{15}CH_3$. Successive models differ by a $TiCl_3$ unit, indicated by the darkest atoms in the figure.

tively, for a series of the small models of increasing size, and the largest models studied, $Ti_{20}Cl_{61}CH_3$ and $Ti_{20}Cl_{60}CH_3$, are illustrated in Fig. 3. The edge-type active sites consist of a five-coordinated titanium atom (four bridging chlorine atoms and a methyl group) and one vacancy, while the metal atom in the corner-type active sites is coordinated to one dangling and two bridging chlorine atoms, a methyl group, and has two vacancies. It has been proposed [21] that the more open aspect of the corner-type active site will give rise to lower regiospecificity in the case of propylene insertion. Details of the geometrical parameters used are given in

Table 1
Bond lengths and angles used in the active site models and active site–ethylene complexes studied in this work. The distance Ti–(C=C) represents the distance from the active Ti to the center of the ethylene C=C bond

Bond lengths (Å)	
Ti–Cl	2.40
Ti–C (alkyl)	2.32
C–H	1.08
C–C	1.35
Ti–(C=C)	2.50
Bond angles (degrees)	
H–C–Ti	110.5
H–C–C	120.0
Cl–Ti–Cl	90.0

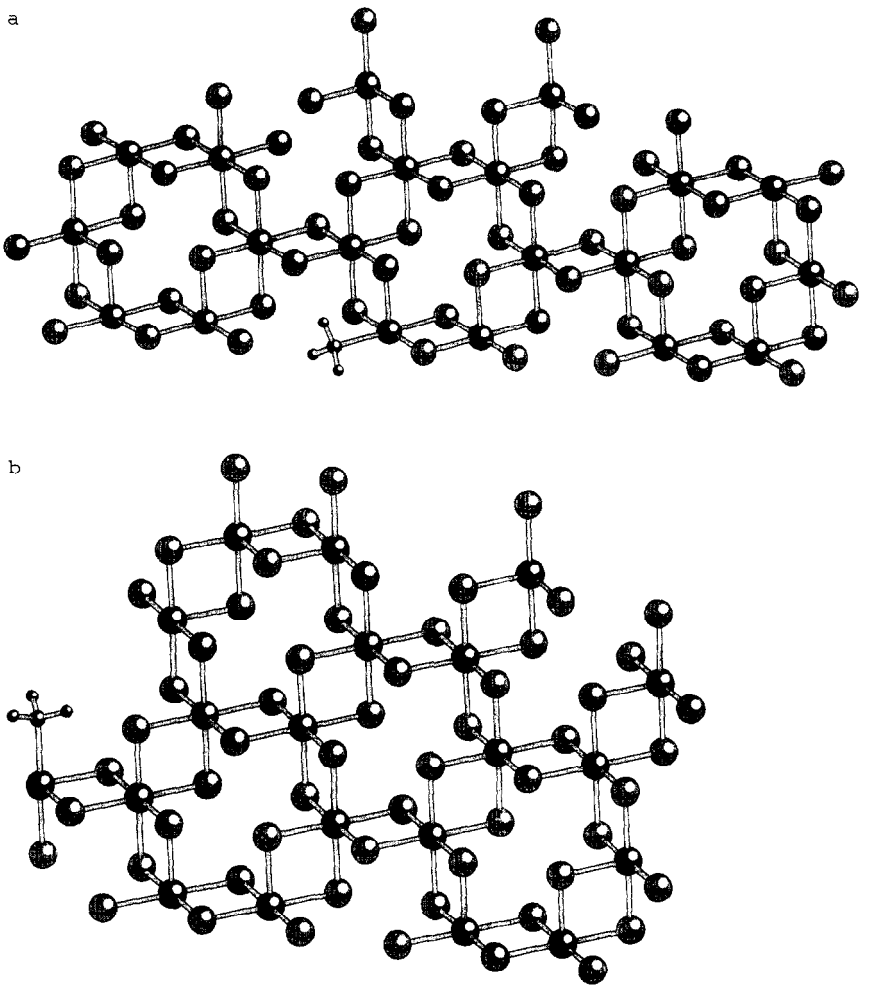

Fig. 3. (a) $Ti_{20}Cl_{61}CH_3$ and (b) $Ti_{20}Cl_{60}CH_3$, the largest edge and corner-type active site models on the surface of α-$TiCl_3$ considered in this work.

Table 1, and the orientations assumed for the ethylene monomer in the initial coordination step to the edge and corner-type sites are shown in Fig. 4.

2.2. Giambiagi–Mayer bond orders

To assist in the interpretation of the results of the extended Hückel calculations in terms of more chemical concepts, the coordination between the active site and the ethylene monomer were analyzed in terms of the bond orders to give an indication of the interactions between atoms according to the scheme of Giambiagi and Mayer [19,20]. This scheme has the attractive feature that for the extended Hückel method it gives *chemically* correct bond orders for diatomic molecules, that is one for H_2, zero for

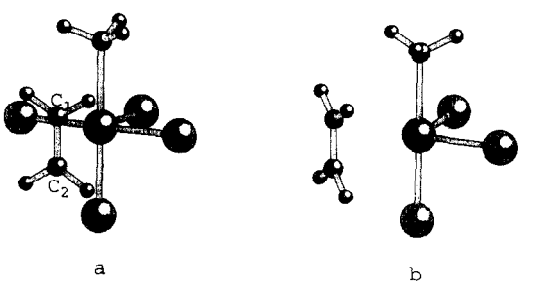

Fig. 4. Models of the active site–ethylene complexes for the (a) edge, and (b) corner-type active site models. Details of the geometrical parameters used are given in Table 1.

He_2, three for N_2, ... (this is also the case for the analysis applied to minimal basis, ab initio HF calculations).

The bond order between two atoms A and B, B_{AB}, in the closed shell case is defined as

$$B_{AB} = \sum_{\mu \in A} \sum_{\nu \in B} (\mathbf{PS})_{\mu\nu}(\mathbf{PS})_{\nu\mu}$$

where $\boldsymbol{P}$, $\boldsymbol{S}$, μ and ν are the density matrix, overlap matrix, and atomic orbitals centered on atoms A and B, respectively.

3. Results and discussion

In this section, firstly we treat the results obtained for the edge-type active sites, and subsequently for the corner-type active sites. Details concerning the extended Hückel parameters used in our calculations can be found in Appendix A.

3.1. Edge-type active sites

The total energies, energies per $TiCl_3$ unit, and Mulliken charges on the active titanium atom for edge-type active site models from $TiCl_4CH_3$ to $Ti_{20}Cl_{61}CH_3$ are presented in Table 2. As the size of the system increases, the positive charge on the active center ($Ti^{\dagger}$) decreases in general. In the cluster containing a single titanium atom, all the four chlorine atoms are unbridged. On addition of a $TiCl_3$ unit, two of these chlorine atoms become bridging atoms, leaving the two others free. This can perhaps explain the small difference between the charge on the active titanium atoms for these two systems ($TiCl_4CH_3$: $q_{Ti^{\dagger}} = 3.371|e^-|$; $Ti_2Cl_7CH_3$: $q_{Ti^{\dagger}} = 3.338|e^-|$). It is only in the cluster containing three or more titanium atoms that all the chlorines in the vicinity of the active site are bridged, which corresponds to the situation in the $TiCl_3$ crystal. At this point there is a sharp decrease in the positive charge on the active site ($Ti_3Cl_{10}CH_3$: $q_{Ti^{\dagger}} = 2.736|e^-|$; $Ti_4Cl_{13}CH_3$: $q_{Ti^{\dagger}} = 2.327|e^-|$). This decrease in positive charge, corresponding to an increase in the number of electrons, on the active site can be accounted for by the fact that a bridging chlorine atom will attract electrons from its two neighboring titanium atoms, while a non-bridging chlorine will attract more strongly the electrons from a single metal atom.

Table 2
Total energies, total energies per $TiCl_3$ unit added ($\Delta TE = TE(Ti_nCl_{3n+1}CH_3) - TE(Ti_{n-1}Cl_{3(n-1)+1}CH_3)$), and Mulliken charges on the active titanium atom for model edge-type active sites of increasing size ($TiCl_4CH_3$–$Ti_{20}Cl_{61}CH_3$) calculated using the extended Hückel method. Energies in eV and charges in $|e^-|$

	Total energy	ΔTE	Charge on active Ti ($Ti^{\dagger}$)
$TiCl_4CH_3$	−631.954		3.371
$Ti_2Cl_7CH_3$	−1026.04	−394.09	3.338
$Ti_3Cl_{10}CH_3$	−1416.05	−390.01	2.736
$Ti_4Cl_{13}CH_3$	−1806.04	−389.99	2.327
$Ti_5Cl_{16}CH_3$	−2195.78	−389.74	2.216
$Ti_6Cl_{19}CH_3$	−2585.51	−389.73	2.284
$Ti_7Cl_{22}CH_3$	−2975.52	−390.01	2.153
$Ti_8Cl_{25}CH_3$	−3365.15	−389.63	2.307
$Ti_9Cl_{28}CH_3$	−3755.26	−390.11	2.435
$Ti_{10}Cl_{31}CH_3$	−4145.02	−389.76	2.419
$Ti_{11}Cl_{34}CH_3$	−4534.91	−389.89	2.123
$Ti_{12}Cl_{37}CH_3$	−4924.73	−389.82	1.547
$Ti_{13}Cl_{40}CH_3$	−5314.74	−390.01	1.464
$Ti_{14}Cl_{43}CH_3$	−5704.38	−389.64	1.653
$Ti_{15}Cl_{46}CH_3$	−6094.51	−390.13	1.653
$Ti_{16}Cl_{49}CH_3$	−6484.26	−389.75	1.518
$Ti_{17}Cl_{52}CH_3$	−6874.15	−389.89	1.579
$Ti_{18}Cl_{55}CH_3$	−7263.96	−389.81	1.553
$Ti_{19}Cl_{58}CH_3$	−7653.49	−389.53	1.656
$Ti_{20}Cl_{61}CH_3$	−8042.95	−389.46	1.749

It should be noted that even for the largest systems studied neither the charge on the active center nor the total energy per $TiCl_3$ unit have converged yet to an asymptotic value, both showing oscillatory behavior. This is a result both of the limited size of the cluster and of the method of increasing the size of the cluster: the disposition of the chlorine atoms in successive $TiCl_3$ units added are not necessarily equivalent, and the number of chlorine bridges formed or dangling chlorine atoms added at each step are not the same.

The total energies, complexation energies,

Table 3
Total energies, complexation energies, Mulliken charges for selected atoms and selected Giambiagi–Mayer bond orders for model edge-type active site–ethylene complexes calculated using the extended Hückel method. Energies in eV and charges in $|e^-|$

	Total energy	$E_{complex}$	Atomic charges			Bond orders			
			q_{Ti^+}	q_{C_1}	q_{C_2}	Ti^+–Me	Ti^+–C_1	Ti^+–C_2	C=C
$TiCl_4CH_3 + C_2H_4$	−845.778	−0.957	3.636	−0.130	−0.163	−0.076	−0.159	−0.155	2.001
$Ti_2Cl_7CH_3 + C_2H_4$	−1239.90	−0.99	3.598	−0.148	−0.165	0.111	−0.159	−0.142	2.009
$Ti_3Cl_{10}CH_3 + C_2H_4$	−1630.78	−1.86	3.322	−0.474	−0.479	0.118	−0.060	−0.053	1.508
$Ti_4Cl_{13}CH_3 + C_2H_4$	−2021.45	−2.54	2.970	−0.794	−0.787	0.122	0.270	0.280	1.195
$Ti_5Cl_{16}CH_3 + C_2H_4$	−2411.19	−2.54	2.813	−0.794	−0.787	0.121	0.270	0.280	1.195
$Ti_6Cl_{19}CH_3 + C_2H_4$	−2800.93	−2.55	2.927	−0.796	−0.789	0.124	0.270	0.278	1.195

atomic charges on selected atoms, and selected bond orders for the complexes formed by the model active sites and ethylene for the systems $TiCl_4CH_3$ to $Ti_6Cl_{19}CH_3$ are presented in Table 3. Unlike the results obtained for the active site models alone, convergence in the results with respect to the size of the system is observed. It is for this reason that we limit the results presented to the smaller systems only. In the case of the clusters containing one and two titanium atoms, the calculated interaction energy is small (−0.96 and −0.99 eV, respectively), the carbon–carbon double bond in the ethylene monomer remains double (values of the Giambiagi–Mayer bond order for the olefin carbon–carbon bond, $B_{C=C}$, equal to 2.001 and 2.009), and negative bond orders exist between the active center and the olefin carbons. The cluster $Ti_3Cl_{10}CH_3$ represents an intermediate situation, and beyond this there is a clear increase in the interaction energy between the cluster and the monomer compared to the smallest systems, which is near constant ($\simeq$ 2.55 eV). Additionally, there is a near-constant transfer of charge to the olefin carbons ($q_C \simeq -0.80|e^-|$ for these systems, compared to $q_C \simeq -0.15|e^-|$ for $TiCl_4CH_3$), a significant decrease in the double bond character of the ethylene carbon–carbon bond ($B_{C=C} = 1.195$), and an increase in the interaction between the active site and the olefin carbons ($B_{Ti-C} \simeq 0.27$).

The significant differences in the results observed for the smallest and all larger model clusters deserve some explanation. Table 4 lists the energies of the two highest occupied, and lowest unoccupied molecular orbitals, and the Mulliken population of the d_{xy} orbital of the active center, which has the correct symmetry to overlap with the π^* antibonding orbital of the olefin, for both the isolated active site models and the active site–ethylene complexes. In the first two clusters, the active titanium d_{xy} orbital

Table 4
Energies of the highest occupied and lowest unoccupied orbitals, and Mulliken population of the active titanium d_{xy} orbital of isolated edge-type active site models and active site + ethylene complexes calculated with the extended Hückel method. Energies in eV and charges in $|e^-|$

	Active site model				Active site + ethylene complex			
	HOMO − 1	HOMO	LUMO	$q_{d_{xy}}$	HOMO − 1	HOMO	LUMO	$q_{d_{xy}}$
$TiCl_4CH_3$	−12.441	−11.931	−7.845	0.013	−12.440	−11.912	−8.574	0.013
$Ti_2Cl_7CH_3$	−12.285	−11.906	−7.874	0.014	−12.265	−11.895	−8.577	0.014
$Ti_3Cl_{10}CH3$	−11.905	−7.895	−7.871	0.533	−11.893	−8.578	−7.867	0.332
$Ti_4Cl_{13}CH_3$	−11.896	−7.903	−7.879	0.793	−11.887	−8.578	−7.882	0.650
$Ti_5Cl_{16}CH_3$	−7.904	−7.883	−7.879	0.865	−8.577	−7.889	−7.877	0.650
$Ti_6Cl_{21}CH_3$	−7.900	−7.890	−7.881	0.637	−8.575	−7.890	−7.884	0.648

Table 5
Total energies, total energies per $TiCl_3$ unit added ($\Delta TE = TE(Ti_nCl_{3n}CH_3) - TE(Ti_{n-1}CH_{3(n-1)}CH_3)$), and Mulliken charges on the active titanium atom for model corner-type active sites of increasing size ($TiCl_3CH_3$–$Ti_{20}Cl_{60}CH_3$) calculated using the extended Hückel method. Energies in eV and charges in $|e^-|$

	Total energy	ΔTE	Charge on active Ti ($Ti^\dagger$)
$TiCl_3CH_3$	−517.024		3.417
$Ti_2Cl_6CH_3$	−906.976	−389.95	2.637
$Ti_3Cl_9CH_3$	−1296.69	−389.72	2.097
$Ti_4Cl_{12}CH_3$	−1686.61	−389.92	1.898
$Ti_5Cl_{15}CH_3$	−2076.49	−389.88	1.682
$Ti_6Cl_{18}CH_3$	−2466.47	−389.98	1.743
$Ti_7Cl_{21}CH_3$	−2856.38	−389.91	1.512
$Ti_8Cl_{24}CH_3$	−3246.14	−389.76	1.503
$Ti_9Cl_{27}CH_3$	−3636.15	−390.04	1.590
$Ti_{10}Cl_{30}CH_3$	−4025.91	−389.76	1.485
$Ti_{11}Cl_{33}CH_3$	−4415.95	−390.04	1.430
$Ti_{12}Cl_{36}CH_3$	−4805.74	−389.79	1.308
$Ti_{13}Cl_{39}CH_3$	−5194.24	−388.50	1.403
$Ti_{14}Cl_{42}CH_3$	−5585.52	−391.28	1.285
$Ti_{15}Cl_{45}CH_3$	−5975.31	−389.79	1.272
$Ti_{16}Cl_{48}CH_3$	−6365.10	−389.79	1.287
$Ti_{17}Cl_{51}CH_3$	−6754.95	−389.85	1.305
$Ti_{18}Cl_{54}CH_3$	−7144.54	−389.59	1.285
$Ti_{19}Cl_{57}CH_3$	−7534.57	−390.03	1.215
$Ti_{20}Cl_{60}.CH_3$	−7924.19	−389.62	1.204

is almost empty, and the LUMOs of these systems are primarily composed of this orbital. For larger clusters containing three and more titanium atoms the occupation of the orbital increases, giving rise to the possibility of back donation to the olefin π^* orbital on coordination. In the active site–ethylene complexes, the LUMO of the two smallest clusters is primarily composed of the ethylene π^* orbital and the active site d_{xy} orbital. For the larger complexes, this orbital is occupied, and the Mulliken population of the titanium d_{xy} orbital is less than in the active site model alone, indicating a transfer of charge towards the π^* orbital of the olefin. Hence, this accounts for the decrease in bond order of the ethylene carbon–carbon bond and the increase in the interaction between the active titanium and the olefin.

3.2. Corner-type active sites

Calculations analogous to those performed on the edge-type active sites were undertaken on the corner-type models. Table 5 lists the total energies, energies per $TiCl_3$ unit, and Mulliken charges on the active center for corner-type active sites from $TiCl_3CH_3$ to $Ti_{20}Cl_{60}CH_3$. There is a similar general decrease in the charge on the active titanium atom to that observed for the edge-type active sites, except that the decrease is already apparent in the cluster containing two titanium atoms. For the corner-type active sites, all the chlorine atoms bridged in the vicinity of the active site in the $TiCl_3$ crystal are already bridged in the $Ti_2Cl_6CH_3$ cluster, and the active site always has one dangling chlorine atom. The overall positive charge on the active site is inferior to that for the edge-type models. Once again, convergence is not reached for the total energies per $TiCl_3$ unit or the Mulliken charge on the active site.

As was the case for the edge-type active site–ethylene complexes, convergence is rapidly

Table 6
Total energies, complexation energies, Mulliken charges for selected atoms and selected Giambiagi–Mayer bond orders for model corner-type active site–ethylene complexes calculated using the extended Hückel method. Energies in eV and charges in $|e^-|$

	Total energy	$E_{complex}$	Atomic charges			Bond orders			
			$q_{Ti^\dagger}$	q_{C_1}	q_{C_2}	$Ti^\dagger$–Me	$Ti^\dagger$–C_1	$Ti^\dagger$–C_2	C=C
$TiCl_3CH_3 + C_2H_4$	−730.903	−1.01	3.647	−0.158	−0.139	0.140	−0.143	−0.138	1.999
$Ti_2Cl_6CH_3 + C_2H_4$	−1121.83	−1.98	3.359	−0.478	−0.471	0.151	−0.054	−0.058	1.502
$Ti_3Cl_9CH_3 + C_2H_4$	−1512.21	−2.69	3.016	−0.790	−0.796	0.157	0.276	0.273	1.191
$Ti_4Cl_{12}CH_3 + C_2H_4$	−1913.93	−14.45	2.141	−0.739	−0.745	0.160	0.275	0.272	1.191
$Ti_5Cl_{15}CH_3 + C_2H_4$	−2292.02	−2.66	2.590	−0.791	−0.796	0.160	0.275	0.272	1.191
$Ti_6Cl_{18}CH_3 + C_2H_4$	−2681.99	−2.65	2.653	−0.791	−0.796	0.160	0.275	0.272	1.191

Table 7
Energies of the highest occupied and lowest unoccupied orbitals, and Mulliken population of the active titanium d_{xy}/d_{xz} orbitals of isolated corner-type active site models and active site + ethylene complexes calculated with the extended Hückel method. Energies in eV and charges in $|e^-|$

	Active site model				Active site + ethylene complex			
	HOMO − 1	HOMO	LUMO	$q_{d_{xy}}$	HOMO − 1	HOMO	LUMO	$q_{d_{xy}/d_{xz}}$
$TiCl_3CH_3$	−12.563	−11.995	−7.863	0.013	−12.560	−11.956	−8.572	0.136
$Ti_2Cl_6CH_3$	−12.981	−7.907	7.879	0.020	−11.950	−8.571	−7.878	0.173
$Ti_3Cl_9CH_3$	−11.962	−7.913	−7.883	0.048	−11.929	−8.568	−7.888	0.330
$Ti_4Cl_{12}CH_3$	−7.919	−7.895	−7.878	0.219	−8.573	−7.892	−7.859	0.428
$Ti_5Cl_{15}CH_3$	−7.920	−7.900	−7.882	0.290	−8.568	−7.907	−7.882	0.510
$Ti_6Cl_{18}CH_3$	−7.905	−7.887	−7.877	0.207	−7.913	−7.887	−7.879	0.479

reached for the complexation energies, bond orders and atomic charges on the olefin carbon atoms for the corner-type active site–ethylene systems, following different behavior for the smallest system. These results are summarized in Table 6 for the corner-site models $TiCl_3CH_3$ to $Ti_6Cl_{18}CH_3$. This can again be analyzed in terms of the difference in occupation with increasing cluster size of the active site d-orbital with the correct symmetry to overlap with the π^* orbital of the incoming olefin (see Table 7), increasing the interaction between the metal and the olefin, and decreasing the strength of the ethylene carbon–carbon bond. The complexation energies of ethylene to both the edge-type and corner-type active sites appear to be similar, with coordination to the corner-type active site slightly more favoured. This is reasonable, qualitatively, given the more open nature of the active titanium. However, these values calculated using the extended Hückel method should be treated with caution and are not reliable in the absolute sense. It should also be remembered that our calculations assume fixed geometries.

4. Conclusion

Our calculations show that care needs to be taken in the choice of models for active sites for heterogeneous Ziegler–Natta polymerization on the $TiCl_3$ crystalline surface. As the size of the model is increased, substantial differences are observed in the net charge of the active titanium atom and, more significantly from the point of view of polymerization, in the nature of interaction with the incoming ethylene monomer. A major increase in the interaction energy with the olefin once the model cluster exceeds a critical size is due to the presence of electrons in low-lying d-orbitals on the active site suitable for back donation into the π^* orbital of the olefin. The parameters considered in the study the ethylene-active site interaction converged rapidly to a near-constant value as the size of the model system was increased.

The role of bridging and non-bridging chlorine atoms appears to be crucial. The presence of non-bridged chlorine atoms on the active site in the smallest models exaggerates the positive charge on the active titanium atom. Mininum models for the corner and edge-type active sites should probably contain at least two and three titanium atoms respectively, sufficient to reproduce the bridging of the chlorine atoms in the vicinity of the active site present in the extended $TiCl_3$ crystal surface. The calculations in this paper suggest that the ideal models should even be slightly larger. In addition to modifying the electronic characteristics of the active titanium atom, the bridging chlorine and adjacent titanium atoms provide potentially valuable constraints on the rigidity of the active site.

The relatively low-level of theory employed here means that the results need to be treated

with some degree of caution. Nevertheless, some valuable indications regarding the nature of the active site on crystalline $TiCl_3$ surfaces and how best to construct suitable models are provided. Work is in progress in our laboratory into the study of the smaller models considered here at the ab initio level.

Acknowledgements

This work has benefitted from the financial support of the Belgian National Interuniversity Research Program on "Sciences of Interfacial and Mesoscopic Structures" (PAI/IUAP No. P3-049). B.C. thanks the Belgian Fund for Scientific Research (FNRS) for his Research Associate Position. All calculations have been performed on the IBM RS6000 Models 730, 560, and 580 of the Namur Scientific Computing Facility (Namur-SCF). The authors gratefully acknowledge the financial support of the FNRS-FRFC, the "Loterie Nationale" for the convention No. 9.4593.92, and the FNRS within the framework of the "Action d'impulsion à la recherche fondamentale" of the Belgian Ministry of Science under the convention D.4511.93.

Appendix A

Calculations in this paper were performed using the program *bind* of the *YAeHMOP* package (Yet Another Extended Hückel Molecular Orbital Package) written by G. Landrum. Information regarding this package is available on the World Wide Web at (http://overlap.chem.cornell.edu:8080/yaehmop.html).

The extended Hückel parameters are given in Table 8.

Table 8

Atom	n	Orbital	VSIE	α_1	c_1	α_2	c_2
H	1	s	−13.6	1.3			
C	2	s	−21.4	1.625			
		p	−11.40	1.625			
Cl	3	s	−24.54	2.250			
		p	−12.97	1.90			
Ti	4	s	−6.82	1.195			
		p	−4.264	0.998			
	3	d	−8.00	4.670	0.3646	1.9861	0.7556

References

[1] T. Simonazzi and U. Giannini, Gaz. Chim. Ital. 124 (1994) 533.
[2] G. Fink, R. Mulhaupt and H.H. Brintzinger (Eds.), Ziegler Catalysts: Recent Scientific Innovations and Technological Improvements, Springer, Berlin, 1995.
[3] P. Cossee, J. Catal. 3 (1964) 80.
[4] P. Corradini, V. Barone, R. Fusco and G. Guerra, Eur. Polym. J. 15 (1979) 1133.
[5] P. Corradini, G. Guerra, R. Fusco and V. Barone, Eur. Polym. J. 16 (1980) 835.
[6] D.R. Armstrong, P.G. Perkins and J.J.P. Stewart, J. Chem. Soc. Dalton Trans. (1972) 1980.
[7] O. Novaro, E. Blaisten-Barojas, E. Clementi, G. Giunchi and M.E. Ruíz, J. Chem. Phys. 68 (1978) 2337.
[8] V.R. Jensen, K.J. Børve and M. Ystenes, J. Am. Chem. Soc. 117 (1995) 4109.
[9] V. Venditto, G. Guerra, P. Corradini and R. Fusco, Polymer 31 (1990) 530.
[10] L. Cavallo, G. Guerra, M. Vacatello and P. Corradini, Macromolecules 24 (1991) 1784.
[11] G. Guerra, L. Cavallo, G. Moscardi, M. Vacatello and P. Corradini, J. Am. Chem. Soc. 116 (1994) 2988.
[12] C.A. Jolly and D.S. Marynick, J. Am. Chem. Soc. 111 (1989) 7968.
[13] H. Weiss, M. Ehrig and R. Ahlrichs, J. Am. Chem. Soc. 116 (1994) 4919.
[14] F.U. Axe and J.M. Coffin, J. Phys. Chem. 98 (1994) 2567.
[15] T.K. Woo, L. Fan and T. Ziegler, Organometallics 13 (1994) 2252.
[16] R. Fusco and L. Longo, Macromol. Theory Simul. 3 (1994) 895.
[17] R.J. Meier, G.H.J. Van Doremaele, S. Iarlori and F. Buda, J. Am. Chem. Soc. 116 (1994) 7274.
[18] V.R. Jensen, M. Ystenes, K. Wärnmark, B. Åkermark, M. Svensson, P.E.M. Siegbahn and M.R.A. Blomberg, Organometallics 13 (1994) 282.
[19] M. Giambiagi, M. Giambiagi, D.R. Grempel and C.D. Heymann, J. Chim. Phys. 72 (1975) 15.
[20] I. Mayer, Chem. Phys. Lett. 97 (1983) 270; Chem. Phys. Lett. 117 (1985) 396 (addendum).
[21] A. Shiga, H. Kawamura-Kuribayashi and T. Sasaki, J. Mol. Catal. A 98 (1995) 15.